

Spin-pumping and Enhanced Gilbert Damping in Thin Magnetic Insulator Films

André Kapelrud and Arne Brataas

Department of Physics, Norwegian University of Science and Technology, NO-7491 Trondheim, Norway

Precessing magnetization in a thin film magnetic insulator pumps spins into adjacent metals; however, this phenomenon is not quantitatively understood. We present a theory for the dependence of spin-pumping on the transverse mode number and in-plane wave vector. For long-wavelength spin waves, the enhanced Gilbert damping for the transverse mode volume waves is twice that of the macrospin mode, and for surface modes, the enhancement can be ten or more times stronger. Spin-pumping is negligible for short-wavelength exchange spin waves. We corroborate our analytical theory with numerical calculations in agreement with recent experimental results.

PACS numbers: 76.50.+g, 75.30.Ds, 75.70.-i, 75.76.+j, 75.78.-n

Metallic spintronics have been tremendously successful in creating devices that both fulfill significant market needs and challenge our understanding of spin transport in materials. Topics that are currently of great interest are spin transfer and spin-pumping [1–3], spin Hall effects [4], and combinations thereof for use in non-volatile memory, oscillator circuits, and spin wave logic devices. A recent experimental demonstration that spin transfer and spin-pumping can be as effective in magnetic insulators as in metallic ferromagnetic systems was surprising and has initiated a new field of inquiry [5].

In magnetic insulators, no moving charges are present, and in some cases, the dissipative losses associated with the magnetization dynamics are exceptionally low. Nevertheless, when a magnetic insulator is placed in contact with a normal metal, magnetization dynamics induce spin-pumping, which in turn causes angular momentum to be dumped to the metal's itinerant electron system. Due to this non-local interaction, the magnetization losses become enhanced. Careful experimental investigations of spin-pumping and the associated enhanced magnetization dissipation were recently performed, demonstrating that the dynamic coupling between the magnetization dynamics in magnetic insulators and spin currents in adjacent normal metals is strong. Importantly, in magnetic insulators, an exceptionally low intrinsic damping combined with good material control has enabled the study of spin-pumping for a much larger range of wave vectors than has previously been obtained in metallic ferromagnets [5–14].

In thin film ferromagnets, the magnetization dynamics are strongly affected by the long-range dipolar interaction, which has both static and spatiotemporal contributions. This yields different types of spin waves. When the in-plane wavelength is comparable to the film thickness or greater, the long-range dipolar interaction causes the separation of the spin-wave modes into three classes depending on the relative orientation of the applied external field, in relation to the film normal, and the spin-wave propagation direction [15–20]. These spin waves are classified according to their dispersion and transverse magnetization distribution as forward volume magneto-

static spin waves (FVMSWs) when the external field is out-of-plane, backward volume magnetostatic spin waves (BVMSWs) when the external field is in-plane and along the direction of propagation, and magnetostatic surface waves (MSSWs) when the external field is in-plane but perpendicular to the direction of propagation. In volume waves, the magnetic excitation is spatially distributed across the entire film, while surface modes are localized near one of the surfaces. “Backward” waves have a frequency dispersion with a negative group velocity for some wavelengths. While these spin waves have been studied in great detail over the last decades, the effect of an adjacent normal metal on these waves has only recently been investigated.

Experimentally, it has been observed that spin-pumping differs for FVMSWs, BVMSWs and MSSWs and that it depends on the spin-wave wavelength [6, 8, 9, 12–14]. Recent experiments [8] have demonstrated that the magnetization dissipation is larger for surface spin waves in which the excitation amplitude is localized at the magnetic insulator-normal metal interface. To utilize spin-pumping from thin film magnetic insulators into adjacent normal metals, a coherent theoretical picture of these experimental findings must be developed and understood, which is the aim of our work.

In this Letter, we present a theory for energy dissipation from spin-wave excitations in a ferromagnetic insulator (FI) thin film via spin-pumping when the ferromagnetic insulator layer is in contact with a normal metal (NM). To this end, consider a thin film magnetic insulator of thickness L on an insulating substrate with a normal metal capping (see Figure 1). We consider a normal metal such as Pt at equilibrium, where there is rapid spin relaxation and no back-flow of spin currents to the magnetic insulator. The normal metal is then a perfect spin sink and remains in equilibrium even though spins are pumped into it.

The magnetization dynamics are described by the Landau-Lifshitz-Gilbert (LLG) equation [21] with a torque originating from the FI/NM interfacial spin-

pumping [22]

$$\dot{\mathbf{M}} = -\gamma \mathbf{M} \times \mathbf{H}_{\text{eff}} + \frac{\alpha}{M_S} \mathbf{M} \times \dot{\mathbf{M}} + \boldsymbol{\tau}_{\text{sp}}, \quad (1)$$

where α is the Gilbert damping coefficient, M_S is the saturation magnetization, γ is the gyromagnetic ratio, \mathbf{H}_{eff} is the effective field including the external field, exchange energy, surface anisotropy energy, and static and dynamic demagnetization fields.

Spin-pumping through interfaces between magnetic insulators and normal metals gives rise to a spin-pumping induced torque that is described as [2]

$$\boldsymbol{\tau}_{\text{sp}} = \frac{\gamma \hbar^2}{2e^2 M_S^2} g_{\perp} \delta\left(\xi - \frac{L}{2}\right) \mathbf{M} \times \dot{\mathbf{M}}, \quad (2)$$

where g_{\perp} is the transverse spin (“mixing”) conductance per unit area at the FI/NM interface. We disregard the imaginary part of the mixing conductance because this part has been found to be small at FI/NM interfaces [12]. In addition, the imaginary part is qualitatively less important and only renormalizes the gyromagnetic ratio.

Assuming only uniform magnetic excitations, “macrospin” excitations, the effect of spin-pumping on the magnetization dissipation is well known [2, 3]. Spin-pumping leads to enhanced Gilbert damping, $\alpha \rightarrow \alpha + \Delta\alpha_{\text{macro}}$, which is proportional to the FI/NM cross section because more spin current is then pumped

out, but inversely proportional to the volume of the ferromagnet that controls the total magnetic moment:

$$\Delta\alpha_{\text{macro}} = \frac{\gamma \hbar}{4\pi L M_S} \frac{h}{e^2} g_{\perp}. \quad (3)$$

Thus, the enhanced Gilbert damping due to spin-pumping is inversely proportional to the film thickness L and is important for thin film ferromagnets. However, a “macrospin” excitation, or the FMR mode, is only one out of many types of magnetic excitations in thin films. The effect of spin-pumping on the other modes is not known, and we provide the first analytical results for this important question, which is further supported and complemented by numerical calculations.

We consider weak magnetic excitations around a homogenous magnetic ground state pointing along the direction of the internal field $\mathbf{H}_i = H_i \hat{\mathbf{z}}$, which is the combination of the external applied field and the static demagnetizing field [19]. We may then expand $\mathbf{M} = M_S \hat{\mathbf{z}} + \mathbf{m}_{Q,xy}(\xi) e^{i(\omega t - Q\xi)}$, where $\mathbf{m}_{Q,xy} \cdot \hat{\mathbf{z}} = 0$, $|\mathbf{m}_{Q,xy}| \ll M_S$, and Q is the in-plane wave number in the ξ -direction.

Following the linearization approach of the LLG equation (1) as in Ref. [19], we arrive at a two-dimensional integro-differential equation of the dynamic magnetization (in the xy -plane) in the film’s transverse coordinate ξ :

$$\left[i \frac{\omega}{\omega_M} \begin{pmatrix} \alpha & -1 \\ 1 & \alpha \end{pmatrix} + \mathbb{1} \left(\frac{\omega_H}{\omega_M} + 8\pi \frac{\gamma^2 A}{\omega_M^2} \left[Q^2 - \frac{d^2}{d\xi^2} \right] + i\alpha \frac{\omega}{\omega_M} \right) \right] \mathbf{m}_{Q,xy}(\xi) = \int_{-\frac{L}{2}}^{\frac{L}{2}} d\xi' \hat{\mathcal{G}}_{xy}(\xi - \xi') \mathbf{m}_{Q,xy}(\xi'), \quad (4)$$

where ω is the spin-wave eigenfrequency, A is the exchange stiffness, $\omega_H = \gamma H_i$, $\omega_M = 4\pi\gamma M_S$, and $\hat{\mathcal{G}}_{xy}$ is the dipole-dipole field interaction tensor, which fulfills the boundary conditions resulting from Maxwell’s equations (see [23]).

The eigensystem must be supplemented by boundary conditions that account for spin-pumping and surface anisotropy. These boundary conditions are obtained by integrating Eq. (1) over the interface [24] and expanding to the lowest order in the dynamic magnetization. When an out-of-plane easy axis surface anisotropy is present, the boundary conditions are

$$\left(L \frac{\partial}{\partial \xi} + i\omega\chi + \frac{LK_s}{A} \cos(2\theta) \right) m_{Q,x}(\xi) \Big|_{\xi=\frac{L}{2}} = 0, \quad (5a)$$

$$\left(L \frac{\partial}{\partial \xi} + i\omega\chi + \frac{LK_s}{A} \cos^2(\theta) \right) m_{Q,y}(\xi) \Big|_{\xi=\frac{L}{2}} = 0, \quad (5b)$$

where K_s is the surface anisotropy energy with units $\text{erg} \cdot \text{cm}^{-2}$ and $\chi = \frac{L\hbar^2 g_{\perp}}{4Ae^2}$ is a parameter relating the ex-

change stiffness and the spin mixing conductance ($[\chi] = \text{s}$). The boundary condition at the magnetic insulator–substrate interface at $\xi = -L/2$ is similar to Eq. (5), but simpler because $\chi \rightarrow 0$ and $K_s \rightarrow 0$ at that interface.

A mathematical challenge induced by spin-pumping arises because the second term in the linearized boundary condition (5) is proportional to the eigenvalue ω such that the eigenfunctions cannot simply be expanded in the set of eigenfunctions obtained when there is no spin-pumping or dipolar interaction. Instead, we follow an alternative analytical route for small and large wave vectors. Furthermore, we numerically determine the eigenmodes with a custom-tailored technique, where we discretize the differential equation (4), include the spin-pumping boundary conditions (5), and transform the resulting equations into an eigenvalue problem in ω [25].

Let us now outline how we obtain analytical results for small $QL \ll 1$ and large $QL \gg 1$ wave vectors. First, we consider the case of vanishing surface anisotropy and compute the renormalization of the Gilbert damping for

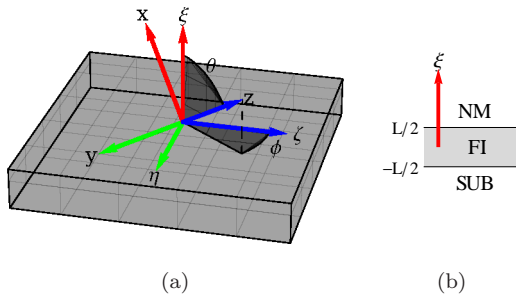


FIG. 1. a) A thin film magnetic insulator of thickness L in its coordinate system; ξ is the normal axis, the infinite $\eta\zeta$ -plane is coplanar with the interfaces, and the spin waves propagate along the ζ -axis. The internal field and saturation magnetization are along the z -axis. The y -axis is always kept in-plane, and the x -axis is selected such that the x -, y - and z -axes form a right-handed coordinate system. b) A cross-section showing the material stack.

the resulting modes. Next, we demonstrate that the surface anisotropy creates a surface wave with a comparably large enhancement of the Gilbert component.

When $QL \ll 1$, the convolution integral on the right-hand side of Eq. (4) only contains the homogeneous demagnetization field. The magnetization is then a transverse standing wave $\mathbf{m}_{Q,xy} (e^{ik\xi} + e^{-ik\xi+\phi})$, where k is a transverse wave number, ϕ is a phase determined by the BC at the lower interface, and the two-dimensional coefficient vector $\mathbf{m}_{Q,xy}$ allows for elliptical polarization in the xy -plane.

By employing exchange-only boundary conditions [24] at the lower interface and using Eq. (5) with $K_s = 0$ on the upper interface, the transverse wave number k is determined by $kL \tan kL = i\omega\chi$. Together with the bulk dispersion relation $\omega = \omega(k)$, calculated from Eq. (4), this expression allows us to calculate the magnetic excitation dispersion relation parameterized by the film thickness, the Gilbert damping α , and the transverse conductance g_{\perp} .

When spin-pumping is weak, $\omega\chi$ is small, and the solutions of the transcendental equation can be expanded around the solutions obtained when there is no spin-pumping, $kL = n\pi$, where n is an integer. When $n \neq 0$, we expand to first order in kL and obtain $kL \approx n\pi + i\omega\chi/(n\pi)$. When $n = 0$, we must perform a second-order expansion in terms of kL around 0, which results in $(kL)^2 \approx i\omega\chi$. Using these relations in turn to eliminate k from the bulk dispersion relation while maintaining our linear approximation in small terms and solving for ω , we obtain complex eigenvalues, where the imaginary part is proportional to a renormalized Gilbert damping parameter, $\alpha^* = \alpha + \Delta\alpha$. When $n = 0$, our results agree with the spin-pumping-enhanced Gilbert damping of the macrospin (FMR) mode derived in [2]

(see Eq. (3)), $\Delta\alpha_0 = \Delta\alpha_{\text{macro}}$. When $n \neq 0$, we compute

$$\Delta\alpha_n = 2\Delta\alpha_{\text{macro}}. \quad (6)$$

These new results indicate that *all* higher transverse volume modes have an enhanced magnetization dissipation that is twice that of the macrospin mode. Thus, counterintuitively, with the exception of the macrospin mode, increasingly higher-order standing-wave transverse spin-wave modes have precisely the same enhanced Gilbert damping.

Next, let us discuss spin-pumping for surface waves induced by the presence of surface anisotropy. When $K_s \neq 0$, the lowest volume excitation mode develops into a spatially localized surface wave. Expanding the expression for the localized wave to the highest order in LK_s/A , we determine after some algebra that the resulting enhancement of the Gilbert damping is

$$\Delta\alpha_{n=0} = \frac{\gamma\hbar K_s}{4\pi M_s A} \frac{h}{e^2} g_{\perp} \frac{\omega_H}{\omega_M} \left[\frac{\omega_H}{\omega_M} + \frac{1}{2} - \frac{K_s^2}{4\pi M_s^2 A} \right]^{-1}. \quad (7)$$

Comparing Eqs. (7) and (6), we see that for large surface anisotropy $LK_s/A \gg 1$, the spin-pumping-induced enhanced Gilbert damping is independent of L . This result occurs because a large surface anisotropy induces a surface wave with a decay length A/K_s , which replaces the actual physical thickness L as the effective thickness of the magnetic excitations, i.e., for surface waves $L \rightarrow A/K_s$ in the expression for the enhanced Gilbert damping of Eq. (3). This replacement implies that the enhanced Gilbert damping is much larger for surface waves because the effective magnetic volume decreases. For typical values of A and K_s , we obtain an effective length $A/K_s \sim 10$ nm. Compared with the film thicknesses used in recent experiments, this value corresponds to a tenfold or greater increase in the enhancement of the Gilbert damping. In contrast, for the volume modes ($n \neq 0$), we note from Eq. (5) that the dynamic magnetization will decrease at the FI/NM interface due to the surface anisotropy; hence, $\Delta\alpha$ decreases compared with the results of Eq. (6).

Finally, we can also demonstrate that for large wave vectors $QL \gg 1$, the excitation energy mostly arises from the in-plane (longitudinal) magnetization texture gradient. Consequently, spin-pumping, which pumps energy out of the magnetic system due to the transverse gradient of the magnetization texture, is much less effective and decays as $1/(QL)^2$ with respect to Eq. (3).

To complement our analytical study, we numerically computed the eigenfrequencies $\omega_n(Q)$. The energy is determined by the real part of $\omega_n(Q)$, while $\text{Im}\omega_n(Q)$ determines the dissipation rate and hence the spin-pumping contribution. Recent experiments [6, 11, 13, 14] on controlling and optimizing the ferrimagnetic insulator yttrium-iron-garnet (YIG) have estimated that the mixing conductances of both YIG—Au and YIG—Pt bilayers

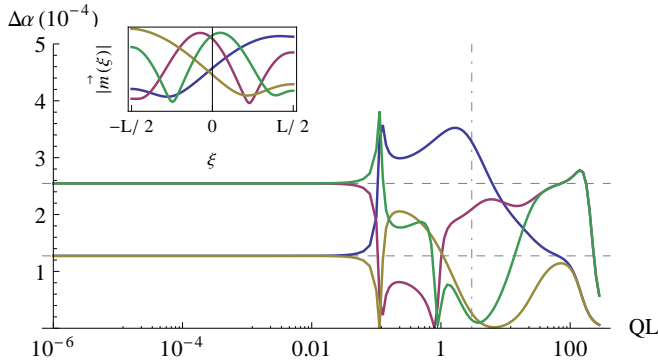


FIG. 2. $\Delta\alpha$ versus wave vector for the MSSW geometry ($\theta = \phi = \pi/2$) for the four lowest eigenvalues. Inset: Magnitudes of eigenvectors (in arbitrary units) across the film at $QL = 1.5$.

are in the range of $g_{\perp}h/e^2 \sim 0.02\text{--}3.43 \cdot 10^{15} \text{ cm}^{-2}$. We use $g_{\perp}h/e^2 = 1.2 \cdot 10^{14} \text{ cm}^{-2}$ from Ref. [6] in this work. All of our results can be linearly re-scaled with other values of the mixing conductance. In the following section, we also use $A = 2.9 \cdot 10^{-8} \text{ erg/cm}$, $K_s = 0.05 \text{ erg/cm}^2$, $L = 100 \text{ nm}$, $4\pi M_S = 1750 \text{ G}$, and $\alpha = 3 \cdot 10^{-4}$.

To distinguish the spin-pumping contribution $\Delta\alpha$ from the magnetization dissipation due to intrinsic Gilbert damping α , we first compute the eigenvalues, ω_d , with intrinsic Gilbert damping, $\alpha \neq 0$, and no spin-pumping, $g_{\perp} = 0$. Second, we compute the eigenvalues ω_{sp} with dissipation arising from spin-pumping only, $\alpha = 0$ and $g_{\perp} \neq 0$. Because $\Im m \omega_d \propto \alpha$, we define a measure of the spin-pumping-induced effective Gilbert damping as $\Delta\alpha = \alpha \Im m \omega_{sp} / \Im m \omega_d$.

We first consider the case of no surface anisotropy. Figure 2 shows the spin-pumping-enhanced Gilbert damping $\Delta\alpha$ as a function of the product of the in-plane wave vector and the film thickness QL in the MSSW geometry. In the long-wavelength limit, $QL \ll 1$, the numerical result agrees precisely with our analytical results of Eq. (6). The enhanced Gilbert damping of all higher transverse modes is exactly twice that of the macrospin mode. In the dipole-exchange regime, for intermediate values of QL , the dipolar interaction causes a small asymmetry in the eigenvectors for positive and negative eigenfrequencies because modes traveling in opposite directions have different magnitudes of precession near the FI/NM interface [26], and spin-pumping from these modes therefore differ. This phenomenon also explains why the enhanced damping, $\Delta\alpha$, splits into different branches in this regime, as shown in Fig. 2. For exchange spin waves, $QL \gg 1$, the exchange interaction dominates the dipolar interaction and removes mode asymmetries. We also see that $\Delta\alpha \rightarrow 0$ for large QL , in accordance with our analytical theory.

Figure 3 shows $\Delta\alpha$ for the BVMSW geometry. The eight first modes are presented; however, as no substantial asymmetry exists between eigenmodes traveling in

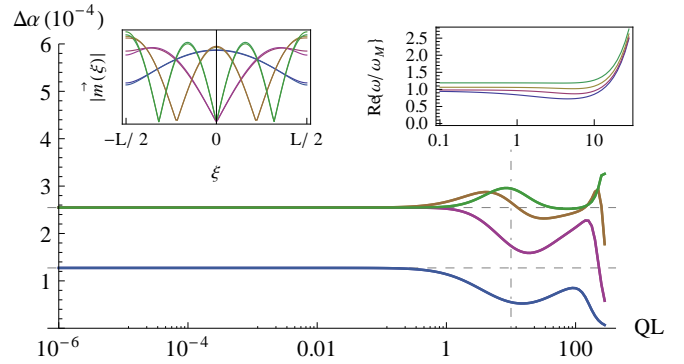


FIG. 3. $\Delta\alpha$ versus wave vector for the BVMSW geometry ($\theta = \pi/2$ and $\phi = 0$). Left inset: Magnitude of eigenvectors (in arbitrary units) across the film when $QL = 1.5$. Right inset: The real part of the dispersion relation for the same modes.

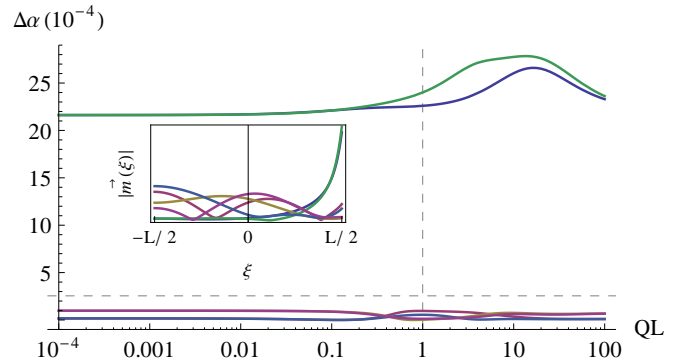


FIG. 4. $\Delta\alpha$ versus wave vector for the MSSW geometry ($\theta = \phi = \pi/2$) with surface anisotropy added at the interface. Inset: Magnitudes of eigenvectors (in arbitrary units) across the film.

different directions, the modes have the same pairwise renormalization of α . This symmetry occurs because the direction of the internal field coincides with the direction of propagation. As in the previous case, the dipolar interaction causes a slight shift in the eigenvectors in the intermediate QL regime, thereby altering $\Delta\alpha$ from that of Eq. (6).

Figure 4 shows $\Delta\alpha$ for the MSSW geometry but with surface anisotropy at the FI/NM interface. As expected from our analytical results, surface anisotropy induces two localized surface modes with a ten-fold larger enhancement of $\Delta\alpha$ compared with the volume modes. The horizontal dashed line in Figure 4 indicates the analytical result for the enhanced Gilbert damping of the $n \neq 0$ modes when $K_s = 0$. For the volume modes, it is clear that the eigenvectors have a lower magnitude closer to the FI/NM interface and that $\Delta\alpha$ is lower compared with the case of $K_s = 0$, which is consistent with our analytical analysis.

Our results also agree with recent experiments. Sandweg *et al.* [8] found that spin-pumping is signifi-

cantly higher for surface spin waves compared with volume spin-wave modes. In addition, in Ref. [9], exchange waves were observed to be less efficient at pumping spins than dipolar spin waves, which is consistent with our results. Furthermore, our results are consistent with the theoretical finding that spin-transfer torques preferentially excite surface spin waves with a critical current inversely proportional to the penetration depth [27].

In conclusion, we have analyzed how spin-pumping causes a wave-vector-dependent enhancement of the Gilbert damping in thin magnetic insulators in contact with normal metals. In the long-wavelength limit, our analytical results demonstrate that the enhancement of the Gilbert damping for all higher-order volumetric modes is twice as large as that of a macrospin excitation. Importantly, surface anisotropy-pinned modes have a Gilbert renormalization that is significantly and linearly enhanced by the ratio LK_s/A .

A. Kapelrud would like to thank G. E. W. Bauer for his hospitality at TU Delft. This work was supported by EU-ICT-7 contract No. 257159 “MACALO”.

-
- [1] A. Brataas, A. D. Kent, and H. Ohno, *Nat. Mater.* **11**, 372 (2012).
- [2] Y. Tserkovnyak, A. Brataas, and G. E. W. Bauer, *Phys. Rev. Lett.* **88**, 117601 (2002).
- [3] Y. Tserkovnyak, A. Brataas, G. E. W. Bauer, and B. I. Halperin, *Rev. Mod. Phys.* **77**, 1375 (2005).
- [4] T. Jungwirth, J. Wunderlich, and K. Olejnik, *Nat. Mater.* **11**, 382 (2012).
- [5] Y. Kajiwara, K. Harii, S. Takahashi, J. Ohe, K. Uchida, M. Mizuguchi, H. Umezawa, H. Kawai, K. Ando, K. Takanasahi, S. Maekawa, and E. Saitoh, *Nature* **464**, 262 (2010).
- [6] B. Heinrich, C. Burrowes, E. Montoya, B. Kardasz, E. Girt, Y.-Y. Song, Y. Sun, and M. Wu, *Phys. Rev. Lett.* **107**, 066604 (2011).
- [7] C. Burrowes, B. Heinrich, B. Kardasz, E. A. Montoya, E. Girt, Y. Sun, Y.-Y. Song, and M. Wu, *Appl. Phys. Lett.* **100**, 092403 (2012).
- [8] C. W. Sandweg, Y. Kajiwara, K. Ando, E. Saitoh, and B. Hillebrands, *Appl. Phys. Lett.* **97** (2010).
- [9] C. W. Sandweg, Y. Kajiwara, A. V. Chumak, A. A. Serga, V. I. Vasyuchka, M. B. Jungfleisch, E. Saitoh, and B. Hillebrands, *Phys. Rev. Lett.* **106**, 216601 (2011).
- [10] L. H. Vilela-Leao, A. A. C. Salvador, and S. M. Rezende, *Appl. Phys. Lett.* **99**, 102505 (2011).
- [11] S. M. Rezende, R. L. Rodriguez-Suarez, M. M. Soares, L. H. Vilela-Leao, D. L. Dominguez, and A. Azevedo, *Appl. Phys. Lett.* **102**, 012402 (2013).
- [12] X. Jia, K. Liu, X. K., and G. E. W. B. Bauer, *EPL* **96**, 17005 (2011).
- [13] M. B. Jungfleisch, V. Lauer, R. Neb, A. V. Chumak, and B. Hillebrands, *ArXiv e-prints* (2013), arXiv:1302.6697 [cond-mat.mes-hall].
- [14] Z. Qiu, K. Ando, K. Uchida, Y. Kajiwara, R. Takahashi, T. An, Y. Fujikawa, and E. Saitoh, *ArXiv e-prints* (2013), arXiv:1302.7091 [cond-mat.mes-hall].
- [15] J. R. Eshbach and R. W. Damon, *Phys. Rev.* **118**, 1208 (1960).
- [16] R. Damon and J. Eshbach, *J. Phys. Chem. Solids* **19**, 308 (1961).
- [17] H. Puzskarski, *IEEE Trans. Magn.* **9**, 22 (1973).
- [18] R. E. D. Wames and T. Wolfram, *J. Appl. Phys.* **41**, 987 (1970).
- [19] B. A. Kalinikos and A. N. Slavin, *J. Phys. C* **19**, 7013 (1986).
- [20] A. Serga, A. Chumak, and B. Hillebrands, *J. Phys. D* **43**, 264002 (2010).
- [21] T. Gilbert, *Phys. Rev.* **100**, 1243 (1955).
- [22] Gaussian (cgs) units are employed throughout.
- [23] B. A. Kalinikos, *Sov. Phys. J.* **24**, 719 (1981).
- [24] G. Rado and J. Weertman, *J. Phys. Chem. Solids* **11**, 315 (1959).
- [25] A. Kapelrud and A. Brataas, Unpublished.
- [26] Z. Wang, Y. Sun, M. Wu, V. Tiberkevich, and A. Slavin, *Phys. Rev. Lett.* **107**, 146602 (2011).
- [27] J. Xiao and G. E. W. Bauer, *Phys. Rev. Lett.* **108**, 217204 (2012).